

Double multiple stream tube theory coupled with dynamic stall and wake correction for aerodynamic investigation of vertical axis wind turbine

Ngoc Anh Vu*, Ngoc Son Pham



Use your smartphone to scan this QR code and download this article

ABSTRACT

This study describes an effectively analytic methodology to investigate the aerodynamic performance of H vertical axis wind turbine (H-VAWT). An in-house code based on double multiple stream tube theory (DMST) coupled with dynamic stall and wake correction is implemented to estimate the power coefficient. Design optimization of airfoil shape is conducted to study the influences of the dynamic stall and turbulent wakes. Airfoil shape is universally investigated by using the Class/Shape function transformation method. The airfoil study shows that the upper curve tends to be less convex than the lower curve in order to extract more energy of the wind upstream and generate less drag of the blade downstream. The optimal results show that the power coefficient increases by 6.5% with the new airfoil shape.

Key words: VAWT, H – rotor, DMST, Dynamic stall, wake correction, Design optimization of the blade

INTRODUCTION

A wind turbine is a turbomachine that converts wind's energy to electrical energy through the use of blades. The type of wind turbine is determined by the direction of the inflow parallel or perpendicular to the axis of rotation. Two major types of wind turbines are horizontal-axis wind turbines (HAWTs) and vertical axis wind turbines (VAWTs). HAWTs are the most common wind turbine because of their high power efficiency compared to VAWTs. This type of wind turbine has the generator at the top of a tower and must be placed into the wind by using steering mechanisms such as a wind vane or a wind sensor coupled with a servomotor. HAWTs are lift-based turbines, whereas VAWTs are drag-based (Savonius) type or lift-based (Darrieus) type machines. VAWTs have the rotor shaft placed vertically, the heavy generator and gearbox can be placed on the ground. The main advantages of VAWTs over HAWTs are lower tip speed ratio and omnidirectionality. HAWTs usually operate at tip speed ratios about 6 - 10, whereas VAWTs operate at 1.5 - 4¹. These features of VAWTs result in higher angles of attack, less cost, and less noise. Therefore, VAWTs are desired for installation near residential areas. The feature of the vertical axis of rotation perpendicular to the free stream velocity eliminates the need for a steering mechanism but also results in more complicated aerodynamics, including various

blade angles of attack, dynamic stall, and wake interference. Therefore, the design and analysis of vertical axis wind turbines are still challenging researches. With the advantages of computer, computational fluid dynamics (CFD) has been widely used in many aerodynamic studies. The realistic 3D model of a wind turbine was usually simplified into a 2D analysis where the cross-section of the turbine is mainly considered. Some studies^{2,3} investigated the isolated airfoil shape of HAWT to optimize the lift/drag ratio using diverse optimization methods. However, VAWT blades are designed to better aerodynamic performance at the various angles of attack they went through. The VAWT performance is significantly affected by 3D flows, such as dynamic stall, tip vortices, and wake interference, that cannot be considered in a 2D airfoil analysis. A first attempt of using CFD to simulate the dynamic motion of a vertical turbine blade in a far-field uniform free-stream velocity flow field was performed by Vassberg et al.⁴. Ferreira et al.⁵ presented a CFD analysis of a two-dimensional straight turbine blade to consider the effect of dynamic stall. Marco Raciti Castelli et al.⁶ proposed a horizontal cross-section CFD model to evaluate power efficiency and calculate aerodynamic forces acting on a straight-bladed vertical axis Darrieus wind turbine. The computational domain is discretized into two distinct sub-grids: a rectangular outer zone

Department of Aerospace Engineering,
Ho Chi Minh City University of
Technology, Vietnam

Correspondence

Ngoc Anh Vu, Department of Aerospace Engineering, Ho Chi Minh City University of Technology, Vietnam
Email: vungocanh@hcmut.edu.vn

History

- Received: 2020-05-20
- Accepted: 2020-11-02
- Published: 2020-12-06

DOI : 10.32508/stdj.v23i4.2396



Copyright

© VNU-HCM Press. This is an open-access article distributed under the terms of the Creative Commons Attribution 4.0 International license.



Cite this article : Vu N A, Pham N S. Double multiple stream tube theory coupled with dynamic stall and wake correction for aerodynamic investigation of vertical axis wind turbine. *Sci. Tech. Dev. J.*; 23(4):776-785.

representing the overall calculation domain and a circular inner zone rotating with rotor angular velocity. Wei-Hsin Chen et al.⁷ simulated the power output of two straight-bladed VAWTs through analyzing the influences of five factors of incoming flow angle, tip speed ratio, the spacing of the turbine, rotational direction, and blade angle on the performance of the dual VAWT system. Buchner et al.⁸ investigated dynamic stall by two-dimensional CFD analysis using unsteady URANS equations with the Menter-SST turbulence model over a range of tip speed ratios. Wei Zuo et al.⁹ performed unsteady numerical simulations to investigate the wake structure of VAWTs and the influence on the aerodynamic performance of the downstream turbine.

A review of the main analytical models used for performance investigation and design of straight blade Darrieus VAWT was conducted by¹⁰. According to the review, the most common models are the double multiple stream tube model. Templin¹¹ proposed the single-stream tube model, which is the first and most simple method for the calculation of the performance of a Darrieus-type VAWTs. Wilson and Lissaman¹² improve the single-stream tube model to conduct the multiple stream tube model. In this model, the swept area of the turbine is divided into a series of adjacent parallel stream tubes. Through further studies¹³⁻¹⁶, BEM - based design has been proved to be able of accurate prediction of Darrieus wind turbine performance. This method is the most basic performance prediction currently used in the industrial design of wind turbines. Aerodynamic performance prediction based on momentum theory and blade element theory is presenting the advantage of a low computation. Gabriele Bedon et al.¹⁷ performed the optimization of a Darrieus vertical axis wind turbine using blade element-momentum theory. An extended database generation for symmetric airfoil is implemented by varying thickness ratio and chord length of the cross-section of blades. Different optimizations were performed and proved configurations characterized by improvements in rotor performance in terms of power coefficient and annual energy production. Airfoil shape having an essential role in the performance of VAWT is the motivation of this study. This study describes an effectively analytic methodology to investigate the aerodynamic performance of H vertical axis wind turbine (H-VAWT). The double multiple stream tube theory (DMST) coupled with dynamic stall and wake correction is implemented to estimate the power coefficient. The airfoil shape is universally represented by using the Class/Shape function transformation method. Therefore, the asymmetric airfoil

is also investigated to find the best airfoil shape giving maximum power coefficient. Design optimization of the airfoil shape is conducted to study the influences of the dynamic stall and turbulent wakes.

METHODOLOGY

The geometric parameters of a VAWT investigated in this study are shown in Table 1. All dynamic stall, wake interaction, and design optimization use these parameters for analyses.

Table 1: H – turbine geometry

H-turbine parameters	
N_b	3
Airfoil	NACA0021
R	515mm
c	85.5mm
σ	0.25

Method of Airfoil Shape Representation

An advanced geometry representation method, the Class Function/Shape Function Transformation (CST), is employed to generate airfoil coordinates. Using the CST method, the function of airfoil coordinates is a multiplication of shape function by class function.

$$y(x/c) = C_{N2}^{N1}(x/c)S(x/c) \tag{1}$$

Where $C_{N2}^{N1}(x/c) = (x/c)^{N1}(1 - x/c)^{N2}$: class function

$N1, N2$: exponents

And $S(x/c) = \sum_{i=0}^N [A_i(x/c)^i]$: shape function

The Bernstein polynomials are used to present the shape function.

$$S_i(x) = K_i x^i (1 - x)^{n-i} \tag{2}$$

Where $K \equiv \binom{n}{i} = \frac{n!}{i!(n-i)!}$ represents binomial coefficient, n is the order of Bernstein polynomial, and i the numbers 0 to n.

The advantages of the CST method in comparison with other methods such as Spline, B-Splines, or NURBS are shown in references^{18,19}. The CST can represent airfoil shape very accurately using fewer scalar control parameters.

The class function for the airfoil is given

$$C(x) = x^{0.5}(1 - x) \tag{3}$$

Fourth order Bernstein polynomial is used for airfoil coordinate function

The upper and lower curves are sequentially presented as below.

$$y_l(x) = C(x) [A_{l0}(1-x)^4 + A_{l1}4x(1-x)^3 + A_{l2}6x^2(1-x)^2 + A_{l3}4x^3(1-x) + A_{l4}x^4] \quad (4)$$

$$y_u(x) = C(x) [A_{u0}(1-x)^4 + A_{u1}4x(1-x)^3 + A_{u2}6x^2(1-x)^2 + A_{u3}4x^3(1-x) + A_{u4}x^4] \quad (5)$$

Streamtube model

Templin¹¹ first proposed the single streamtube model for the estimation of Darrieus VAWTs. In this model, a single streamtube encloses the turbine. The induced velocity is constant throughout the disc and is calculated by equating the streamwise force and the change of momentum along the streamtube.

Wilson and Lissaman¹² improved a single stream tube to a multiple stream tube model. The single-stream tube is divided into multiple parallel stream tubes. Each stream tube is independently considered using the blade element and momentum theories to calculate the induced velocity.

Double multiple stream tube (DMST), the employed method in this study, is proposed by Paraschivoiu¹⁶. The turbine is considered as two separate actuator disks, which are the front and rear half-cycle. In Figure 1, the cross section ∞ denotes the plane far upstream of the turbine (free stream). Cross-section 1 and 2 are sequentially the planes at the upwind and downwind actuator disk. Cross-section e is the equilibrium flow, which is considered to be far enough from both disks. Cross-section w is the wake far from disk 2. The swept area of jth stream tube with infinitesimal angular width δθ can be calculated from Figure 1.

$$A_{1,j} = R\delta\theta \sin \theta_j, \theta_j \in (0, \pi) \quad (6)$$

$$A_{2,j} = R\delta\theta (-\sin \theta_j), \theta_j \in (\pi, 2\pi) \quad (7)$$

The interference factor of the front and rear half cycle are defined:

$$a_1 = V_{a1}/V_\infty \text{ and } a_2 = V_{a2}/V_e \quad (8)$$

The thrust coefficient for the front and rear half-cycle is sequentially expressed:

$$C_{F1} = F_1(0.5\rho A_{1,j}V_\infty^2) \quad (9)$$

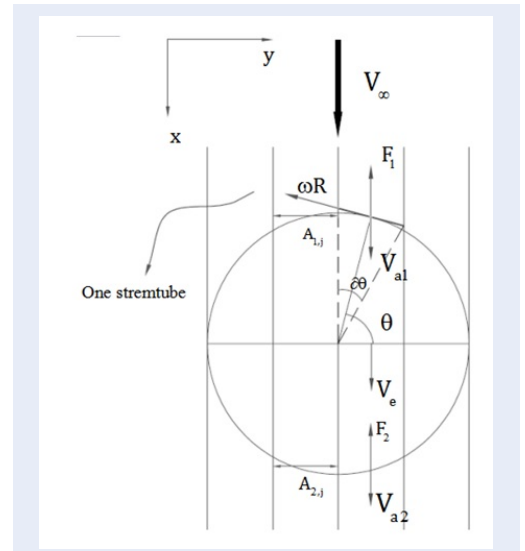


Figure 1: The velocity vector field at the 2D blade.

$$C_{F2} = F_2(0.5\rho A_{2,j}V_e^2) \quad (10)$$

Three conservation laws of fluid mass, momentum, energy are applied to each stream tube and give the thrust coefficient expression:

$$C_{Fi} = 4a_i(1 - a_i), i = 1, 2 \quad (11)$$

Blade element theory for VAWT

A cross-section of the blade is considered. The scheme of the flow velocities and forces at a specific location of the blade is described in Figure 2. The relative velocity VR is a sum of free-stream wind velocity and blade rotating velocity as following.

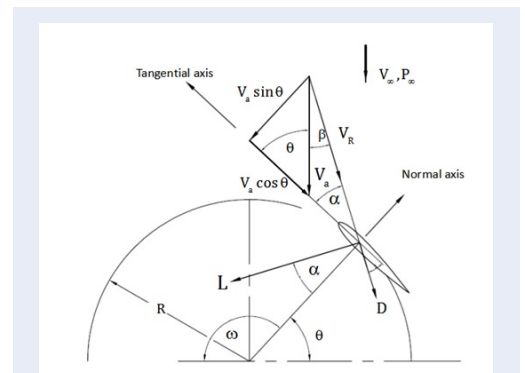


Figure 2: Scheme of flow velocities and forces

$$V_R = \sqrt{(V_a \sin \theta)^2 + (V_a \cos \theta + \omega R)^2} \quad (12)$$

Where V_a is the axial flow velocity through the rotor, θ is the azimuth angle, ω is the rotational velocity of the blade, and R is the radius of the turbine.

Normalizing the relative velocity using free stream wind velocity, it can be expressed as a function of tip speed ratio ($TSR = \omega R / V_\infty$), V_∞ , the azimuth angle θ :

$$\frac{V_R}{V_\infty} = \frac{1}{\sqrt{\left(\frac{V_a}{V_\infty}\right)^2 + TSR^2 + 2\frac{V_a}{V_\infty}TSR\cos\theta}} \quad (13)$$

The relative angle of attack and moving path angle can be expressed as:

$$\alpha = \tan^{-1} \left(\frac{\frac{V_a}{V_\infty} \sin \theta}{\frac{V_a}{V_\infty} \cos \theta + TSR} \right), \quad (14)$$

$$\beta = \tan^{-1} \left(\frac{TSR \sin \theta}{\frac{V_a}{V_\infty} + TSR \cos \theta} \right)$$

The instantaneous thrust at any given azimuthal angle can be obtained:

$$F_i(\theta_{i,j}) = 0.5\rho c V_{R,i}^2 \times (C_D \cos \beta - C_L \sin \beta); \quad i = 1, 2 \quad (15)$$

Therefore, the force time-averaged along one period in one single stream tube for N_b blades of the turbine can be calculated:

$$F_i = \frac{N_b}{2\pi} \int_{\theta_{i,j} - \delta\theta/2}^{\theta_{i,j} + \delta\theta/2} F_i(\theta) d\theta \approx \frac{N_b \delta\theta}{2\pi} F_i(\theta_{i,j}); \quad i = 1, 2 \quad (16)$$

Therefore, the thrust coefficient at each stream tube can be expressed:

$$C_{F1} = \frac{\sigma}{\pi \sin \theta} \frac{V_{R,1}^2}{V_\infty^2} \times (C_D \cos \beta - C_L \sin \beta)$$

$$C_{F2} = -\frac{\sigma}{\pi \sin \theta} \frac{V_{R,2}^2}{V_\infty^2 (2a_2 - 1)} \times (C_D \cos \beta - C_L \sin \beta) \quad (17)$$

Where, the solidity is defined as $\sigma = N_b c / (2R)$

Calculation of power coefficient

The thrust coefficients calculated from DMST and BET are equal. Following the converged solution of the thrust coefficient, the interference factors of the front and rear half cycle, α, β can be computed.

The blade torque coefficient at any given azimuthal angle can be calculated

$$C_{Q_b}(\theta) = -\frac{V_R^2}{V_\infty^2} [\cos \theta (C_D \cos \theta - C_L \sin \theta) + \sin \theta (C_D \sin \theta + C_L \cos \theta)] \quad (18)$$

The total power coefficient of all blades can be calculated by expression:

$$C_P = C_{P,1} + C_{P,2} \quad (19)$$

Where:

$$C_{P,1} = C_{P,front} = \frac{\sigma TSR}{2\pi} \int_0^\pi C_{Q_b} d\theta,$$

$$C_{P,2} = C_{P,rear} = \frac{\sigma TSR}{2\pi} \int_0^{2\pi} C_{Q_b} d\theta \quad (20)$$

The overall flow chart of the calculation of the power coefficient is presented in Figure 3.

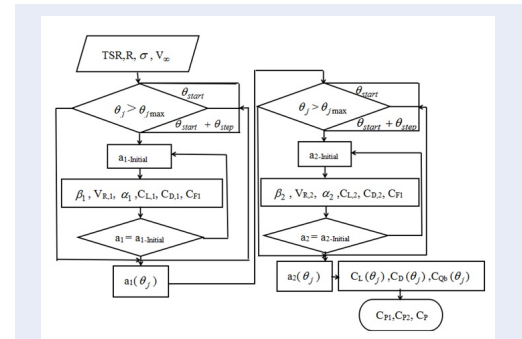


Figure 3: Calculating algorithm of power coefficient.

Dynamic stall model

Dynamic stall is an unsteady aerodynamic phenomena that occurs when the blade rapidly changes the angle of attack (AoA). This plays a very important role in performance of VAWTs in which the AoA of individual blade periodically changes, particularly at low tip-speed ratios. Dynamic stall presents a hysteresis behavior of the flow passing through the blades, whereas the flow does not immediately react to the variation of AoA.

When the airfoil angle of attack is increasing rapidly, the flow passing upper surface of airfoil is pressed toward its surface and remains substantially attached

to the airfoil. As a result, the stall is delayed and an achieved lift coefficient is significantly higher than the steady state maximum.

In the model of Gormont²⁰, the reference AoA after applying a delay $\delta\alpha$ is

$$\alpha_{ref} = \alpha - K\delta\alpha \quad (21)$$

where K is a correction factor proposed by Gormont:

$$K = \begin{cases} 1 : \dot{\alpha} \geq 0 \\ -0.5 : \dot{\alpha} < 0 \end{cases} \quad (22)$$

The delay, $\delta\alpha$, is empirical function of the airfoil thickness and Mach number of the flow:

$$\delta\alpha = \begin{cases} \gamma_1 S : S \leq S_c \\ \gamma_1 S + \gamma_2 (S - S_c) : S > S_c \end{cases} \quad (23)$$

where $S = \sqrt{\frac{c\dot{\alpha}}{2V_R}}$ is non-dimensional rate ratio, $S_c = 0.006 + 1.5(0.006 - \frac{t}{c})$ is a function of airfoil thickness, γ is a function of airfoil thickness and Mach number.

Finally, the modified lift coefficient is calculated:

$$C_L^{dyn} = C_{L,0}(\alpha_0) + m(\alpha - \alpha_0) \quad (24)$$

Where m is the minimum value of either the slope of the linear part of CL or the value of the expression:

$$\left(C_{L,0}(\alpha_{ref}) - C_{L,0}(\alpha_0) \right) / (\alpha_{ref} - \alpha_0) \quad (25)$$

The modified drag coefficient is obtained by using α_{ref} to take the data from the static one.

$$C_D^{dyn} = C_D(\alpha_{ref}) \quad (26)$$

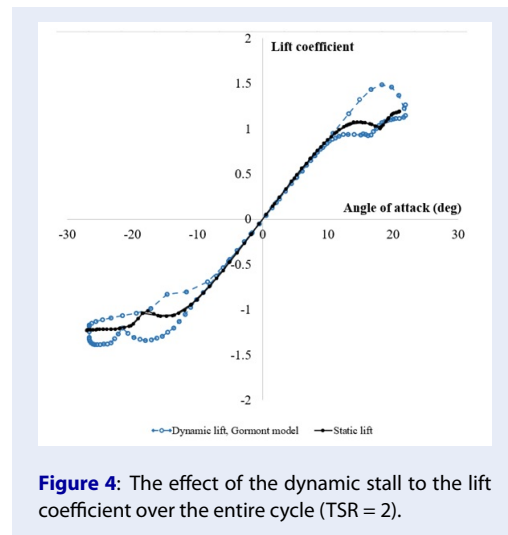


Figure 4: The effect of the dynamic stall to the lift coefficient over the entire cycle (TSR = 2).

Figure 4 shows a comparison of the static and dynamic lift coefficient. They are equal in the linear variation. When the absolute value of AoA is increasing outside the linear regime, the dynamic stall occurs at a higher AoA than the static stall, $\alpha_{ss} \approx 10^\circ$. However, when it is decreasing, the upper surface flow changes its state more easily. Hence the dynamic lift adapts faster to the static value.

Wake interaction

Wake interaction is the effect of the turbulent wakes generated by the front half blades on the rear half blades. By studying graphic visualizations of the vorticity generated by the blades, Kozal et al.²¹ proposed a formula to calculate the number of wakes, $N_\omega = 0.85N_b TSR$. Each blade almost intersect with wake twice. By neglecting the wake diffusion, the wake length can be calculated, $L_{wake} = 2cN_\omega$.

Kozak et al. showed that the flow inside the wake travels at the same speed and direction that the blade generated it. The relative velocity of the flow in the wake is negligible, the AoA within the wake goes to zero. These effects can be distributed evenly throughout the rear half cycle that the blades pass a half circumference. Hence the effective AoA can be corrected:

$$\alpha_{wake}(\theta) = \left(1 - \frac{L_{wake}}{\pi R} \right) \alpha_{ref}(\theta); \quad 180 < \theta < 360 \text{ deg} \quad (27)$$

The change of effective AoA in the front and rear half cycle is illustrated in Figure 5.

As can be seen in Figure 5, the effective AoA estimated by DMST with and without wake correction is coincident in the front half cycle. The effective AoA estimated by the DMST is significantly higher than that of CFD calculation in the rear half cycle.

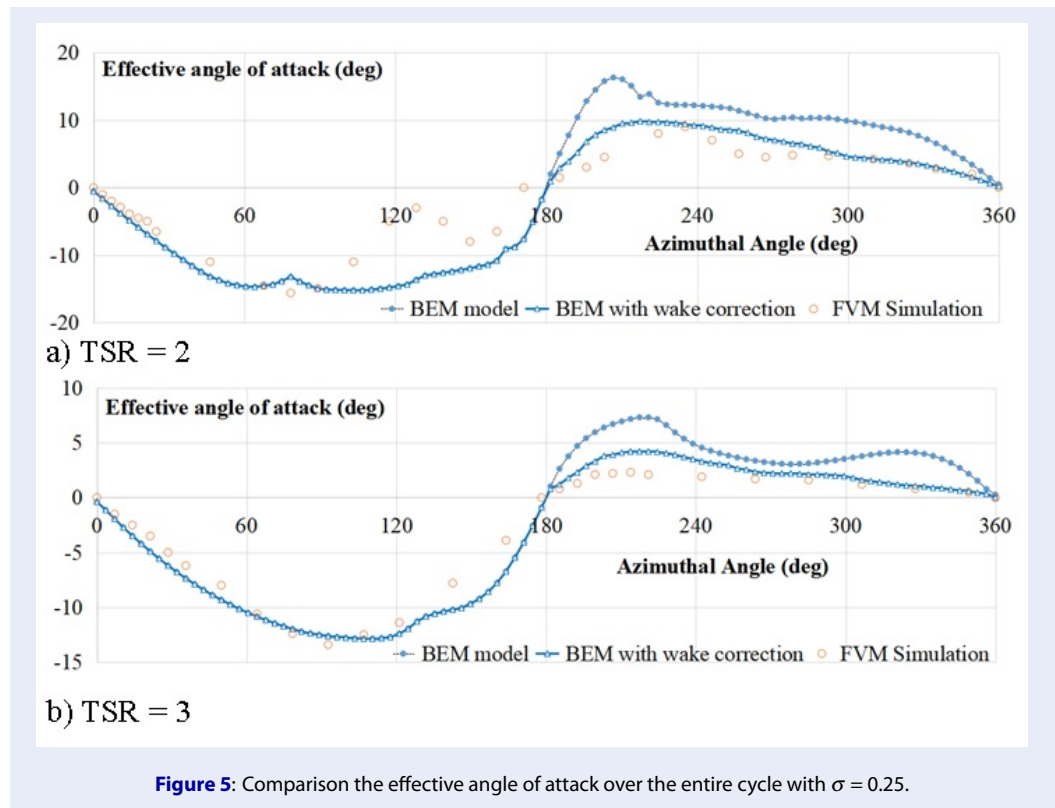
The DMST with wake correction improves the accuracy in estimating effective AoA for the entire range of azimuthal angles between 180-360 deg, particularly at higher tip speed ratios.

The wake correction has different effects responding to tip speed ratio. When the blade collides with the wake in the rear half cycle, its lift and drag coefficient decrease dramatically.

$$C_L^{wake} = \begin{cases} C_L^{dyn} : \theta \in (0, \pi) \\ C_L^{dyn} (1 - r_\omega) : \theta \in (\pi, 2\pi) \end{cases} \quad (28)$$

$$C_D^{wake} = \begin{cases} C_D^{dyn} : \theta \in (0, \pi) \\ C_D^{dyn} (1 - r_\omega) : \theta \in (\pi, 2\pi) \end{cases}$$

Where $r_\omega = \frac{L_{wake}}{\pi R}$ is the proportion of the blade path in the back that cuts a wake.



DESIGN OPTIMIZATION

Validation

In the Figure 6, the average power coefficient calculated by DMST with and without dynamic stall and wake correction is plotted with CFD result conducted by Kozak²¹. Kozak investigated the performance of the VAWT by using finite volume method simulation. The low Y+ treatment at the boundary layer was shown to generate accurate results.

The dynamic stall becomes dominant characteristic at low TSR < 2. The Gormont model implemented in this study improves the accuracy in calculating the power coefficient. As a result, the DMST with dynamic stall correction gets closer to CFD simulation in comparison with DMST itself. The DMST is not able to take into account the wake dynamics dominant at high tip speed ratios. The effects of the wake interaction result in lower AoA, hence lower power output in the rear half cycle.

Design optimization

The airfoil shape is parameterized by using CST method presented in section 2.1. The parameters, $A_{u0}-A_{u4}$ and $A_{l0}-A_{l4}$, sequentially control upper and lower curves of the airfoil shape. Consequently, asymmetric airfoils are also investigated to optimize the

power output of VAWT. The well-known XFOIL program is used to calculate lift and drag coefficients of the airfoil for a wide range of AoA. A preprocessing of airfoil coordinates is applied before running the XFOIL in order to produce convergent lift and drag coefficients. The average power coefficient of the VAWT is chosen as an objective function calculated by DMST with dynamic stall and wake correction. Constraints on design variables, $0 \leq A_{u0} - A_{u4} \leq 0.35$, $-0.35 \leq A_{l0} - A_{l4} \leq 0$ is used to assure success of design optimization. The symmetric baseline airfoil NACA0021 is a pre-optimal result conducted by a number of studies^{6,21,22}. Therefore, the simple gradient-based method is employed to find optimal results quickly.

Figure 7b shows that the baseline airfoil NACA0021 generates positive torque in both the front and rear half cycle, and the blade returns the energy to the flow instead of extracting from it at some portions at ends of the rear half cycle and starts of the front half cycle. When the blade thickness increases, it was demonstrated to delay the onset of the stall at high blade angles of attack but decreases the lift-to-drag ratio. It was observed that a negative camber airfoil resulted in almost all of the energy being extracted at the front half of the turbine cycle. The advanced CST method controls the airfoil shape by 10 design

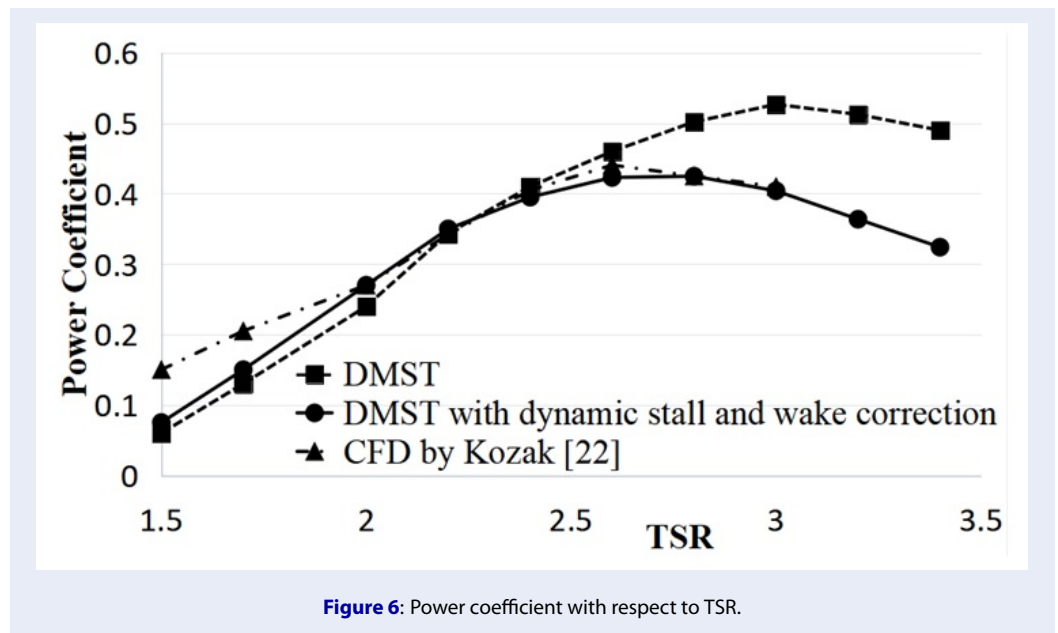


Figure 6: Power coefficient with respect to TSR.

variables that can generate the optimal airfoil without degrading the performance of VAWT in the rear half cycle. Since the airfoil shape is isolatedly searched for the best performance, the optimal airfoil produces more torque, maximum $C_{Q_b} \approx 0.25$ in the front half, whereas the blades are freely rotating in the rear half cycle almost without returning or extracting the energy from the flow. Eventually, the average power coefficient of VAWT improves by 6.5% at considered $TSR = 3$. The optimal airfoil works better at all TSRs as shown in Figure 7c.

The results of optimization design are summarized in Table 2.

CONCLUSION

This study successfully demonstrated a process for optimizing the airfoil shape of the blade. An in-house code using DMST method with dynamic stall and wake correction are developed and proved that it is able to predict the performance of VAWTs properly. The dynamic stall plays essential role at low TSRs, whereas, the wake interaction is dominant at high TSRs. The average power coefficients generated by current study agree well with CFD simulation and be accuracy for design optimization, particularly at the optimal TSR in between 2.5 to 4. The CST method is shown to be a good representation of airfoil shape that give geometric flexibility for searching optimal shape. The negative camber airfoil results in the design that achieved an efficiency 6.5% higher than that of baseline airfoil. The airfoil study shows that upper curve tends to be less convex than the lower curve in order

to extract more energy of the wind upstream and generate less drag of the blade downstream.

In all cases, the VAWT geometry is adjusted to extract maximum energy from flow at the front half cycle but not prevent the rotation of the blades in the rear half cycle.

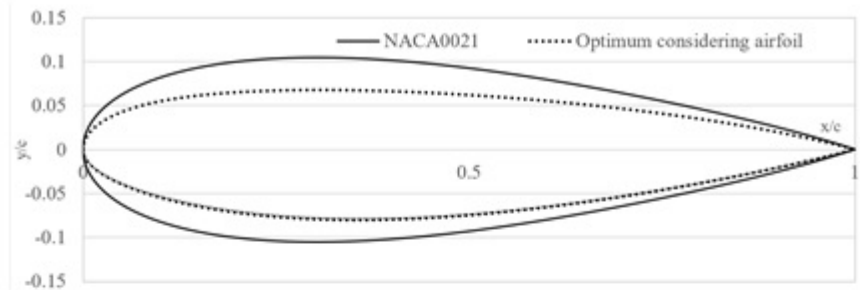
ACKNOWLEDGMENT

This work was supported by the National Foundation for Science and Technology Development (NAFOS-TED) of Vietnam (Project No. 107.01-2017.15).

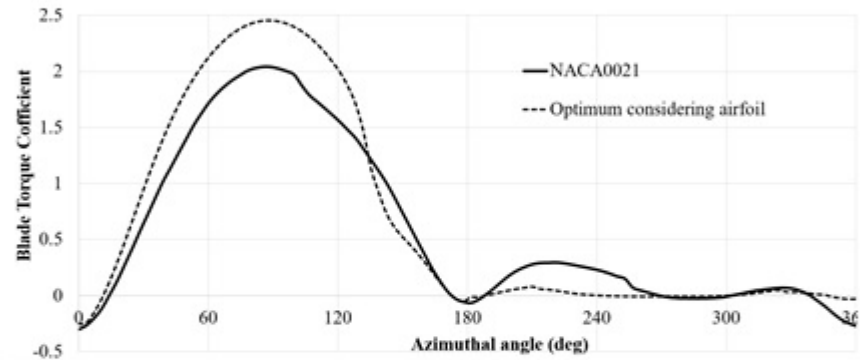
NOMENCLATURE

REFERENCES

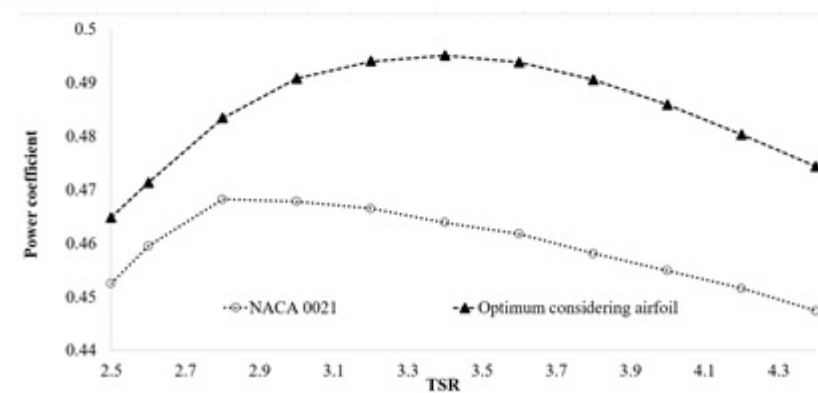
1. Paraschivoiu. Wind Turbine Design: With Emphasis on Darrieus Concept. Polytechnic International Press, Montreal. 2002;p. 66–85.
2. Langtry RB, Gola J, Menter FR. Predicting 2D Airfoil and 3D Wind Turbine Rotor Performance using a transition Model for General CFD Codes. 44th AIAA Aerospace Science and Exhibit, Reno, Nevada, USA. 2006;Available from: <https://doi.org/10.2514/6.2006-395>.
3. Li JY, Li R, Gao Y, Huang J. Aerodynamic optimization of wind turbine airfoils using response surface techniques, Proceeding of the Institution of Mechanical Engineers. Part A: Journal of Power and Energy. 2010;
4. Vassberg JC, Gopinath AK, Jameson A. Revisiting the vertical-axis windturbine design using advanced computational fluid dynamics. 43rd AIAA Aerospace Science and Exhibit. Reno, Nevada, USA. 2005;Available from: <https://doi.org/10.2514/6.2005-47>.



a) Optimal airfoil shape



b) Blade torque coefficient



c) Average power coefficient wrt. TSR of VAWT

Figure 7: Optimal results of airfoil study

5. Ferreira CJS, Bijl H, Bussel G, Kuik G. Simulating dynamic stall in a 2D VAWT: modeling strategy, verification and validation with particle image velocimetry data. *Journal of Physics: Conference Series*. 2007;75. Available from: <https://doi.org/10.1088/1742-6596/75/1/012023>.
6. Castelli MR, Englaro A, Benini E. The Darrieus wind turbine: Proposal for a new performance prediction model based on CFD. *Energy*. 2011;36(8):4919–4934. Available from: <https://doi.org/10.1016/j.energy.2011.05.036>.
7. Chen WH, Chen CY, Huang CY, Hwang CJ. Power output analysis and optimization of two straight-bladed vertical-axis wind turbines. *Applied Energy*. 2017;185(1):223–232. Available from: <https://doi.org/10.1016/j.apenergy.2016.10.076>.
8. Buchner AJ, Lohry MW, Martinelli L, Soria J, Smits AJ. Dynamic stall in vertical axis wind turbines: Comparing experiments and computations. *Journal of Wind Engineering and Industrial Aerodynamics*. 2015;146:163–171. Available from: <https://doi.org/10.1016/j.jweia.2015.09.001>.
9. Zuo W, Wang X, Kang S. Numerical simulations on the wake effect of H-type vertical axis wind turbines. *Energy*. 2016;106:691–700. Available from: <https://doi.org/10.1016/j.energy.2016.02.127>.
10. Islam M, Ting DSK, Fartaj A. Aerodynamic models for Darrieus-type straight-bladed vertical axis wind turbines. *Renewable and Sustainable Energy Reviews*. 2008;12(4):1087–1109. Available from: <https://doi.org/10.1016/j.rser.2006.10.023>.
11. Templin RJ. Aerodynamic performance theory for the NRC vertical-axis wind turbine. Ottawa, National Research Council of Canada; 1976.

Table 2: Design optimization results

		min	max	Baseline	Optimum Considering Airfoil
Design variables	A_{u0}	0	0.35	0.3004	0.2104
	A_{u1}	0	0.35	0.2631	0.1549
	A_{u2}	0	0.35	0.2819	0.1806
	A_{u3}	0	0.35	0.2169	0.1653
	A_{u4}	0	0.35	0.2867	0.2287
	A_{l0}	-0.35	0	-0.3004	-0.1797
	A_{l1}	-0.35	0	-0.2631	-0.2166
	A_{l2}	-0.35	0	-0.2819	-0.2174
	A_{l3}	-0.35	0	-0.2169	-0.2012
	A_{l4}	-0.35	0	-0.2867	-0.2267
Objective function: Average power coefficient C_p				0.465	0.495

cil, Canada. 1974;.

12. Wilson RE, Lissaman PBS. Applied aerodynamics of wind power machines. Oregon State University. 1974;.
13. Read S, Sharpe DJ. An extended multiple streamtube theory for vertical axis wind turbine, Proceeding of the second BWEA wind energy workshop. British wind energy Association. 1980;.
14. Paraschivoiu I. Double-Multiple streamtube model for Darrieus wind turbines, NASA. Lewis Research Center Wind Turbine Dyn. 1981;p. 19–25.
15. Paraschivoiu I, Delclaux F. Double multiple streamtube model with recent Improvements. Journal of Energy. 1983;7(3):250–255. Available from: <https://doi.org/10.2514/3.48077>.
16. Paraschivoiu I. Double-Multiple streamtube model for studying vertical-axis wind turbines. Journal of Propulsion and Power. 1988;4(4):370–377. Available from: <https://doi.org/10.2514/3.23076>.
17. Bedon G, Castelli MR, Benini E. Optimization of a Darrieus vertical-axis wind turbine using blade element momentum theory and evolutionary algorithms. Renewable Energy. 2013;59:184–192. Available from: <https://doi.org/10.1016/j.renene.2013.03.023>.
18. Vu NA, Lee JW, Shu J. Aerodynamic Design Optimization of Helicopter Rotor Blades Including Aerofoil Shape for Hover Performance. Chinese Journal of Aeronautics. 2013;26(1):1–8. Available from: <https://doi.org/10.1016/j.cja.2012.12.008>.
19. Vu NA, Lee JW. Aerodynamic Design Optimization of Helicopter Rotor Blades Including Airfoil Shape for Forward Flight. Aerospace Science and Technology. 2015;42:106–117. Available from: <https://doi.org/10.1016/j.ast.2014.10.020>.
20. Gormont RE. A Mathematical Model of Unsteady Aerodynamics and Radial Flow for Application to Helicopter Rotors. Philadelphia: US, Army Air Mobility R&D Laboratory, Vertol Division. 1973;.
21. Kozak PA, Vallverdú D, Rempfer D. Modeling vertical-axis wind-turbine performance: blade-element method versus finite volume approach. Journal of Propulsion and Power. 2016;32(3):592–601. Available from: <https://doi.org/10.2514/1.B35550>.
22. Carrigan TJ, Dennis BH, Han ZX, Wang BP. Aerodynamic shape optimization of a vertical-axis wind turbine using differential evolution. ISRN Renewable Energy. 2012; Available from: <https://doi.org/10.5402/2012/528418>.

Table 3: Symbol

$A_{l0}-A_{l4}$	Constants of airfoil lower curve polynomial
$A_{u0}-A_{u4}$	Constants of airfoil upper curve polynomial
$A_{1,j}$	The swept area of jth streamtube at the upwind
$A_{2,j}$	The swept area of jth streamtube at the downwind
C_L, C_D	Lift, drag coefficient of the airfoil
C_L^{dyn}, C_D^{dyn}	Dynamic lift, drag coefficient
C_P, C_{P1}, C_{P2}	Total power coefficient, power coefficient of the front half, power coefficient of the rear half
D	Drag
L	Lift
c	Chord length of the turbine blade
N_b	Number of blade
R	Rotor radius
V_{a1}	Axial flow velocity at cross section 1, upstream
V_{a2}	Axial flow velocity at cross section 2, downstream
V_e	Axial flow velocity at cross section e, middle stream
V_∞	Wind velocity at the free stream
α	Angle of attack to blade section
ϕ	Pitch angle
θ	Azimuthal angle
σ	Turbine solidity
ω	Blade rotating velocity
(x, y)	(x, y) of the airfoil coordinates

Table 4: Abbreviations

AoA	Angle of attack
BET	Blade element theory
CST	Class Function/Shape Function Transformation
DMST	Double multiple streamtube theory
DVs	Design variables
HAWT	Horizontal axis wind turbine
TSR	Tip speed ratio
VAWT	Vertical axis wind turbine